Electrochimica Acta 245 (2017) 165–172

Contents lists available at ScienceDirect

Electrochimica Acta

journal homepage: www.elsevier.com/locate/electacta

On the supercapacitor performance of microwave heat treated self organized TiO_2 nanotubes: influence of the cathodic pre-treatment, water aging, and thermal oxide

Diego D. Silva[a], Isaac Sánchez-Montes[a], Peter Hammer[b], José M. Aquino[a,*]

[a] Universidade Federal de São Carlos, Departamento de Química, C.P. 676, 13560-970 São Carlos, SP, Brazil
[b] Universidade Estadual Paulista (UNESP), Instituto de Química de Araraquara, Departamento de Físico-Química, 14800-900 Araraquara, SP, Brazil

ARTICLE INFO

Article history:
Received 13 April 2017
Received in revised form 13 May 2017
Accepted 17 May 2017
Available online 20 May 2017

Keywords:
TiO_2 nanotubes
black TiO_2
microwave oven
supercapacitor
barrier oxide
oxygen vacancy

ABSTRACT

The electrical and morphological properties as well as the assessment of self organized TiO_2 nanotubes (TiO_2-NTs) as supercapacitors were carried out for the first time for samples grown in organic medium and annealed in a microwave oven (MO) through a hybrid thermal heating. These samples were compared to those obtained by heat treatment in a conventional muffle furnace (MF). No significant differences were observed in the nanotubular morphology, crystalline structure (anatase phase) and of the band gap values; however, samples annealed in a MO showed an improvement in the donor density and a higher flat band potential. After a cathodic pre-treatment (–1.4 V *vs.* NHE for 60 s) to generate oxygen vacancies/Ti^{3+} (black TiO_2) the MO annealed samples exhibited a superior areal capacitance than the MF annealed samples, even after 5000 cycles of galvanostatic charge-discharge experiments. The improved performance of the MO annealed samples is related to a higher amount of produced oxygen vacancies/Ti^{3+} on the surface of TiO_2-NT. As the generated surface oxygen vacancies are unstable, reactions with adsorbed H_2O lead to a more hydroxylated surface layer. Electrochemical impedance spectroscopy (EIS) measurements of the as-prepared black TiO_2 exhibited a significant diminishment of the charge transfer resistance for the MO annealed samples; however, assessment of the water aging stability of these pre-treated films resulted in increasing values for the charge transfer resistance. The thermally grown oxide interface layer formed on the Ti substrate showed for both annealing methods similar EIS profiles and seems it has no influence on the values obtained for the areal capacitance. The results suggest that microwave annealing is an interesting option to convert amorphous TiO_2-NTs into the crystalline anatase phase, especially because this procedure is very rapid and facile, resulting in an improvement of their areal capacitance after a cathodic pre-treatment.

1. Introduction

Titanium dioxide (TiO_2) is a versatile material [1] extensively investigated in materials science due to its optical, electrical, and electrochemical properties. The main characteristics that contributes to this is the varying geometries and morphologies [2–4] that TiO_2 can be obtained with high surface to volume ratios, which enable it to be used in many fields such as photocatalysis [5], solar cells [6], and electrochemical energy storage devices [7]. Among those morphologies, the nanotubular one has been claimed to promote a rapid charge carrier separation to hinder recombination [8]. TiO_2 nanotubes (TiO_2-NTs) can be synthesized using different techniques [3], such as hydrothermal and electrochemical. The last one has the advantage to attain a self organized and aligned material [9], without problems of adherence [10], in organic and aqueous media at distinct bath compositions [11]. On the other hand, the as-grown film has to be thermally treated to obtain the desired anatase crystalline phase [12]. Aside the conventional annealing method using the muffle furnace, some other non-conventional methods such as flame annealing [13], hydrothermal-thermal annealing [14], and microwave annealing [15–17] have been reported. Among them, the use of a microwave oven is a faster and simple method to convert the amorphous TiO_2-NTs into crystalline without any detrimental changes to the morphology or

* Corresponding author.Tel.: + 55 16 33066864.
E-mail address: jmaquino@ufscar.br (J.M. Aquino).

http://dx.doi.org/10.1016/j.electacta.2017.05.112
0013-4686/

electrical properties [16]. This facile annealing method is based on a hybrid heating [18] through the use of SiC, which promptly absorbs microwave radiations and convert them to heat.

Presently, the main application of TiO_2-NTs is focused on water treatment or as anode material in electrochemical devices [1]. Concerning the latter application, films of TiO_2-NTs have been used as double layer supercapacitors (DLSC) [19–21], or in combination with other metal oxides [7], mainly due to their high active area [22]; however, high values of capacitance are only achieved when a cathodic pre-treatment is carried out (other reduction processes are also possible [23] using other metallic oxides, such as MoO_3 [24]) before galvanostatic charge-discharge experiments. That behavior, often referred to electrochemical doping, seems to be related with generation of oxygen vacancies and Ti^{3+} sites in the TiO_2 film (resulting in the so called black TiO_2) with a consequent diminishment of the film resistivity [25,26]. In this respect, however, only few works are concerned on how electrochemical properties are affected by the generation of these species in the TiO_2 film as well as their stability on air or in solution. Oxygen vacancies formed on the surface of TiO_2 react readily with adsorbed H_2O leading to hydroxyl groups on its surface [27,28], which can affect the electrocatalytic properties of TiO_2 [29]. Lattice disorder and generation of midgap states has been also reported [30,31] to be associated with reduced TiO_2 nanoparticles resulting in high efficiencies for photocatalytic reactions [32]. In addition, other important factors that are not often investigated in the literature, such as the use of non-conventional annealing methods (for the generation of the anatase phase), may have significant influence on the structure and thus on the performance of reduced TiO_2-NT films as supercapacitor.

Thus, the aim of the present work is to compare the morphological, structural and electrical properties of TiO_2-NT films, grown in organic medium and thermally treated using a microwave oven and muffle furnace. The performance of electrochemically reduced TiO_2-NTs as DLSC using both annealing methods to crystallize the TiO_2 film have been investigated. Furthermore, the influence of the thermally grown oxide over Ti and the effect of long term stability during a water aging process of TiO_2-NT films, after a cathodic pre-treatment, have been investigated through electrochemical impedance spectroscopy.

2. Materials and methods

Initially, Ti plates (99.7%) were sequentially wet-grounded with 320, 400, and 600 SiC abrasive papers. Then, the plates were cleaned for 30 min in an ultrasonic bath containing 2-propanol followed by rinsing with deionized H_2O. The electrochemical anodization (50 V for 60 min) was carried out using a two-electrode conventional cell with the Ti plate as anode (0.5 cm^2) and a Pt foil as cathode under constant stirring at 23 °C. The electrolytic bath was composed of a 0.5% (*m*/*m*) NH_4F (A.R Sigma-Aldrich) solution in ethylene glycol (A.R Panreac, 99.5%, with 0.1% H_2O) with 0.9% (*m*/*m*) deionized H_2O. After anodization, the Ti plates were thoroughly rinsed with deionized H_2O and then dried at ambient conditions. The thermal treatments were carried out using a commercial 2.45 GHz/800 W microwave oven for 3 min and a conventional muffle furnace at 600 °C for 30 min. More information concerning the annealing conditions [15], previously optimized to produce only the anatase phase, as well as the microwave oven setup [33] was reported elsewhere. The maximum measured temperatures (using a non contact infrared thermometer) inside the microwave oven for distinct treatment periods are showed in Fig. SC-1 of the supplementary content file.

The thermally treated TiO_2-NTs were analyzed by: *i*) field-emission scanning electron microscopy (FEI inspect F50), for morphological characterization, *ii*) grazing incidence X-ray diffraction – GIXRD (RU200 B Rigaku Rotaflex, from 20 to 80° at 1° min^{-1}, CuKα 1.5406 Å), for crystalline phase analysis, and *iii*) UV–vis diffuse reflectance (Varian Cary 5G), for optical band-gap energy (E_g) estimation. The effect of different annealing methods and conditions on the electrical properties of the TiO_2-NTs has been characterized by AC impedance measurements in the dark at 1.0, 2.5, 5.0, 7.5, and 10.0 kHz, from −0.2 to 3.0 V *vs.* RHE (reversible hydrogen electrode – the reference electrode was connected to the cell through a salt bridge), with potential steps of 10 mV, using a naturally aerated 0.5 mol L^{-1} H_2SO_4 at ambient temperature in the dark.

The use of thermally treated TiO_2-NTs as supercapacitors was carried out in two steps using a naturally aerated 0.5 mol L^{-1} Na_2SO_4 at ambient temperature. Initially, the annealed TiO_2-NT samples were electrochemically treated at different cathodic potentials (from −1.0 to −1.6 V *vs.* RHE) and treatment times (30 to 120 s). Then, cyclic voltammetry (CV) measurements (100 cycles for each scan rate: from 100 to 1000 mV s^{-1}) were carried out from 0 to 1.0 V *vs.* RHE to analyze the areal capacitance (*C*), according to the equation:

$$C = \frac{(Q_+ + |Q_-|)}{\Delta E\, A} \quad (1)$$

where Q_+ and Q_- are the charges resulting from the anodic and cathodic scans during the CV measurements, $\triangle E$ the potential interval (1.0 V), and *A* the geometric area (~0.5 cm^2). After optimization of the cathodic pre-treatment, charge and discharge galvanostatic (5000 cycles at 100 μA cm^{-2}) experiments were carried out in triplicate from 0 to 1.0 V *vs.* RHE. The areal capacitance obtained during discharge (C_d) for the TiO_2-NT samples thermally treated using a microwave oven and muffle furnace were calculated according to:

$$C_d = \frac{Q_d}{\Delta E\, A} \quad (2)$$

where Q_d is the calculated charge during the discharge. It is important to mention that before the charge-discharge galvanostatic experiments, TiO_2-NT samples were submitted to the cathodic pre-treatment in the optimized conditions followed by CV measurements (10 cycles at 100 mV s^{-1}). A conventional three-electrode cell (TiO_2-NTs, RHE and Pt foil as working, reference and counter electrode, respectively) has been used during all electrochemical experiments, which were carried out in the dark.

The effect of the cathodic pre-treatment on the thermally treated TiO_2-NT samples using a microwave oven and muffle furnace was investigated by *ex situ* X-ray photoelectron spectroscopy (XPS) and AC impedance measurements in the range of 5 kHz to 1 mHz with a perturbation amplitude of 10 mV. The XPS analyses were carried out using samples that were previously subjected to a cathodic pre-treatment in a 0.5 mol L^{-1} Na_2SO_4 solution, dried with N_2 gas, and maintained under vacuum before assays. A commercial spectrometer (UNI-SPECS UHV) operating at a pressure of less than 10^{-7} Pa was used for the measurements. The Al Kα line was used ($h\nu$ = 1486.6 eV) and the analyzer pass energy was set to 10 eV. The inelastic background of the Ti 2p, O 1 s and C 1 s electron core-level spectra was subtracted using Shirley's method. The composition (at.%) of the near surface region was determined with an accuracy of ±10% from the ratio of the relative peak areas corrected by Scofield's sensitivity factors of the corresponding elements. The binding energy scale of the spectra was corrected using the C 1 s hydrocarbon component of the fixed value of 285.0 eV. The spectra were fitted using the CasaXPS software using multiple Voigt profiles without placing constraints. The width at half maximum (FWHM) varied between 1.2 and 2.0 eV and the accuracy of the peak positions was ±0.1 eV. The AC impedance assays were carried in intervals of 1 to 156 h after the

cathodic pre-treatment to assess the effect of aging time on the charge transfer resistance and constant phase element capacitance. All electrochemical impedance spectroscopy measurements were carried out with respect to the open circuit potential. A 0.5 mol L^{-1} Na_2SO_4 solution was used for these experiments that were carried out in the dark. During these measurements, the TiO_2-NT samples were always maintained immersed in the electrolyte, i.e., no drying process was applied after the cathodic pre-treatment.

3. Results and discussion

3.1. Morphological, structural, and electrical characterizations of thermally treated TiO_2-NT

As can be observed from scanning electron microscopy (SEM) micrographs of Fig. 1a and 1b, TiO_2 nanotube tops with an internal diameter of 90 nm remained open after different annealing processes, in comparison to as-grown nanotubes reported previously [15] and also shown in Fig. SC-2. Similar results were also obtained during microwave annealing treatment of TiO_2 nanotubes grown in aqueous medium [16]. This is an important morphological characteristic, since other methods that rapidly convert amorphous TiO_2-NTs to the crystalline anatase phase, such as flame annealing [13] or water aging [34], may lead at some conditions to tube closing. It is also important to mention that these micrographs were representative of the entire surface.

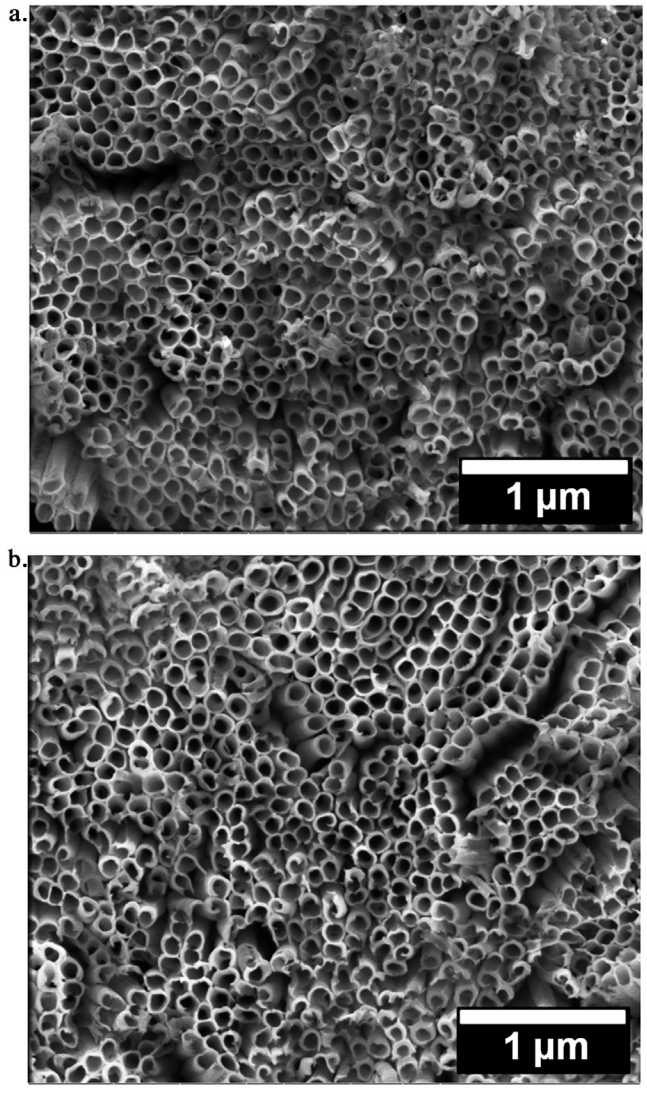

Fig. 1. Secondary electron microscopy images of TiO_2 nanotubes grown in organic medium and thermally treated using a **a)** microwave oven for 3 min and **b)** muffle furnace at 600 °C for 30 min.

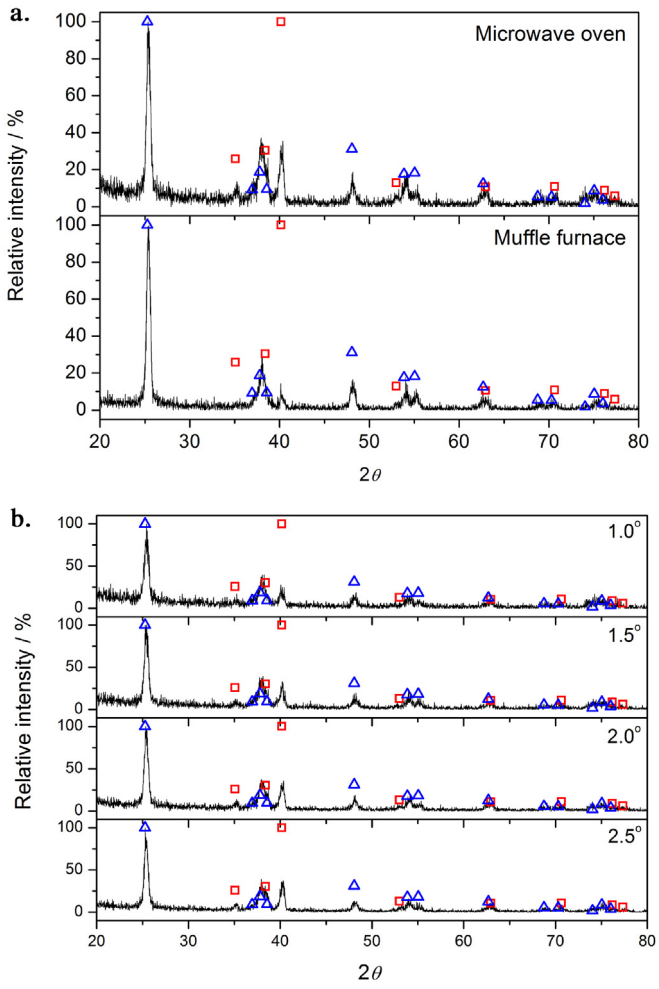

Fig. 2. Grazing incidence X-ray diffraction of TiO_2 nanotube samples **a)** after thermal treatment by microwave and muffle furnace and **b)** only using the microwave oven at different incident angles (from 1.0° to 2.5°). Symbols refer to the diffraction peaks based on the JCPDS cards: (□) Ti (44–1294) and (△) anatase TiO_2 (21–1272).

As can be observed in the X ray diffractograms (GIXRD) of Fig. 2a, the desired anatase crystallographic phase was obtained after thermal treatment using both methods (characteristic (101) peak of the anatase phase at 26°). As expected and according to previous results [15], no peaks of the undesired rutile phase were detected. As discussed in the work of Acevedo-Peña et al. [35] and Albu et al. [36], heat treatments carried out at temperatures higher than 400 °C can induced the formation of the rutile phase due to the thermal oxidation of the underlying Ti or even conversion of the anatase phase of the TiO_2-NT film into the rutile phase, close to the Ti substrate. Consequently, GIXRD experiments were carried out by varying the incident angle, as discussed in ref. [35], to be able to detect a possible formation of the rutile phase close to the Ti substrate. As shown in Fig. 2b, no X ray diffraction peaks of the undesired rutile phase were observed for the microwave annealed TiO_2-NT sample for different incident angles. These results suggest that no appreciable amounts of the rutile phase are present in the TiO_2-NT samples that were heat treated using the microwave oven.

Modified Kubelka-Munck – Tauc $[(F(R) \times h\nu)^{0.5}]$ expression as a function of photon energy was used to estimate of the E_g values for

the TiO_2 nanotubes thermally treated using a microwave oven and muffle furnace (see Fig. SC-3 in the supplementary content file). The extrapolation of the linear part of the curves to the energy axis yielded E_g values of about 3 eV for both samples. As expected, these values are similar to those reported by several authors [3,37,38]. Other methods to estimate the E_g values have been used [39,40] such as a plot of $\ln[(R_{max} - R_{min}/R_d - R_{min})]^n$ as a function of $h\nu$, where R_{max} and R_{min} refer to the maximum and minimum values of diffusive reflectance, R_d is the reflectance at a given $h\nu$, and n is equal to 1/3 for indirect forbidden transition; however, the linear range of the curves was better noticed when using the most common method of the Kubelka-Munk expression. The influence of different annealing methods on the electrical properties of TiO_2-NTs was investigated by AC impedance measurements through analyses of Mott-schottky plots, i.e. $1/C_{SC}^2$ *vs.* E where C_{SC} is the capacitance of the space charge layer and E the applied potential. All procedures and equations to obtain the donor density (N_d) and flat band potential (E_{FB}) were also described in a previous paper [16]. As shown in Fig. SC-4, the Mott-Schottky plots exhibited a positive slope that is typical of n-type semiconductors. The variation of the perturbation frequency from 1 to 10 kHz exhibited a negligible slope increase, as well as a diminishment of the E_{FB} values, which might be related to superficial trapped states or other characteristic of the nanotubular film. This behavior was already noticed for TiO_2-NTs grown in aqueous medium [16] when using Na_2SO_4 as the supporting electrolyte. The obtained N_d values (considering the most common used frequency of 1 kHz for 5 different samples of each annealing treatment) for the thermally treated samples using a microwave oven and muffle furnace were $1.4\ (\pm 0.3) \times 10^{18}\ cm^{-3}$ and $0.4\ (\pm 0.2) \times 10^{18}\ cm^{-3}$, respectively. These results indicate a faster carrier transfer for the microwave oven annealed samples, possibly due to its faster thermal cycle that led to different types of defects in the TiO_2 structure [41]. More information concerning the thermally grown oxide over Ti will be given in section 3.3. Similar results concerning an increase of the N_d values were also reported for TiO_2-NT samples grown in aqueous medium and thermally treated in microwave oven [16]; however, N_d values for samples grown in aqueous medium were one order of magnitude higher than the one for samples grown in organic medium. The E_{FB} values remained around 0.50 (±0.08) V and 0.36 (±0.03) V for the annealed TiO_2-NT samples using a microwave oven and muffle furnace, respectively.

3.2. Effect of different heat treatments on the performance of TiO_2 nanotubes as supercapacitors

The use of thermally treated TiO_2-NTs as supercapacitor was initially investigated considering distinct conditions for a cathodic pre-treatment to increase the film conductivity (possibly by reduction of Ti^{4+} to Ti^{3+} and/or presence of oxygen vacancies) and also the available active area. As can be seen in Fig. 3, higher values of areal capacitance (C) were obtained for a cathodic pre-treatment at −1.4 V during 60 s for the annealed TiO_2-NTs using a microwave oven. For comparison see Fig. SC-5 for TiO_2-NT samples thermally treated using a muffle furnace. The application of lower cathodic potentials and higher treatment times led to a rupture or even dissolution of the nanotubular morphology due to a decrease in the overpotential (more conductive TiO_2-NT film) for the H_2 evolution reaction [16], resulting in low values of areal capacitance. Zhou and Zhang [19] reported a similar cathodic potential applied for the electrochemical doping of TiO_2-NT; however, for a treatment time of more than 10 min. The observed decrease of the areal capacitance with the increase of the scan rate is related to ion accessibility limitation for purely electrical double layer supercapacitors [19]. In addition, the electrochemical doping led to a

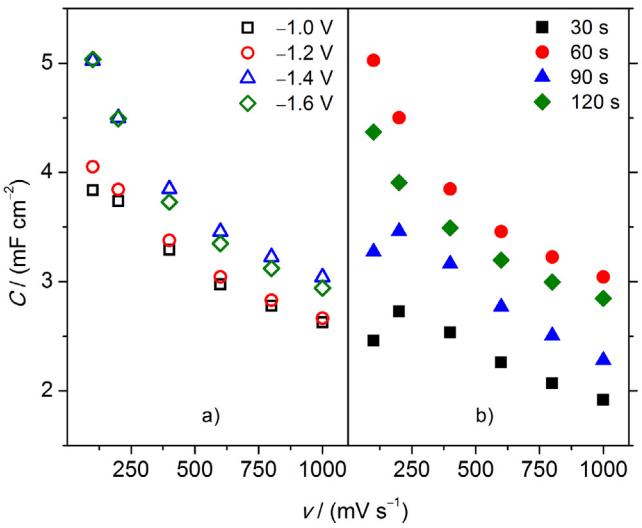

Fig. 3. Areal capacitance (obtained by cyclic voltammetry experiments after the 100° cycle) as a function of the scan rate at **a)** constant time (60 s) and **b)** constant potential (−1.4 V *vs.* NHE) during the cathodic pre-treatment of the TiO_2 nanotube samples thermally treated using a microwave oven. Conditions: 0.5 mol L^{-1} Na_2SO_4 solution in the dark.

film darkening that gradually returned to its original gray color [42], probably due to electron transfer reactions with adsorbed H_2O or dissolved O_2 in solution, as previously observed with air treated TiO_2-NT samples [43]. SEM micrographs obtained after optimization of the cathodic pre-treatment conditions (−1.4 V for 60 s) exhibited no morphological damages of the nanotubular array for both annealing conditions (see Fig. SC-6), except for the increasing number of nanotubes that were detached from each other.

In order to investigate if the cathodic pre-treatment could have led to any modification of the active surface areas of the TiO_2-NT samples annealed using both methods, linear sweep polarizations in the presence of the $[Fe(CN)_6]^{4-}/[Fe(CN)_6]^{3-}$ redox pair were carried out for samples heat treated using the microwave oven and the muffle furnace. Considering the geometric area of the TiO_2-NT samples (0.5 cm^2) and the obtained values of their active surface areas ($1.5 \pm 0.2\ cm^2$ and $1.6 \pm 0.2\ cm^2$ for the microwave oven and muffle furnace treated samples, respectively – for more details see data in Tables SC-1 and SC-2 and Fig. SC–7), the cathodic pre-treatment significantly modifies the active surface areas. On the other hand, the two heat treatment methods have no effect on the value of the enhanced active surface area of the samples.

The characteristic square shape of the cyclic voltammetry curves, shown in Fig. 4, confirmed that the TiO_2-NT electrode behaves as a double layer supercapacitor, as no faradaic peak is observed. A similar behavior is observed for muffle furnace treated TiO_2-NT samples (see Fig. SC-8, in the supplementary content file). Fig. 5 shows the discharge cycle (C_d) dependence of the areal capacitance recorded during galvanostatic charge-discharge assays using a current density of 100 $\mu A\ cm^{-2}$. Clearly, after the cathodic pre-treatment the average C_d values of microwave treated TiO_2-NT are higher than those treated in the muffle furnace. This behavior might be related to the higher amounts of Ti^{3+}/oxygen vacancies produced during the cathodic pre-treatment of samples annealed using a microwave oven, as will be discussed below. It is important to emphasize the crucial role of the cathodic pre-treatment in improving the C_d values of the heat treated TiO_2-NT samples. This is evident when compared with much lower C_d values of not treated samples (empty symbols of Fig. 5) and this might be due to a diminishment of the film resistivity (see section 3.3) due to the formation of band gap states generated by Ti^3

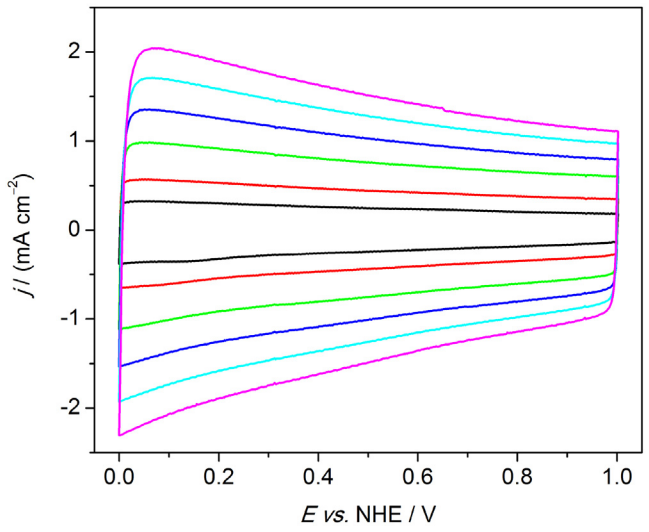

Fig. 4. Cyclic voltammetries (100° cycle) of the TiO_2 nanotube samples thermally treated using a microwave oven for 3 min. The curves were obtained after a cathodic pre-treatment at −1.4 V (*vs.* RHE) for 60 s and using different scan rates: (⬭) 100, (—) 200, (—) 400, (—) 600, (—) 800, and (—) 1000 mV s^{-1}. Conditions: 0.5 mol L^{-1} Na_2SO_4 solution in the dark.

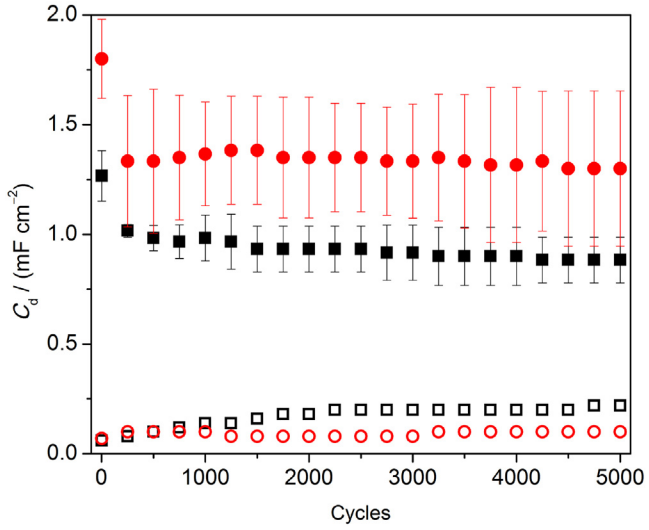

Fig. 5. Areal capacitance obtained during discharge (C_d) as a function of cycle number for the TiO_2-NT samples thermally treated using a microwave oven (● and ○) and muffle furnace (■ and □). The full and empty symbols refer to the samples that were pre-treated at −1.4 V (*vs.* RHE) for 60vs s or not, respectively, and the C_d error bars refer to three different samples of each annealing treatment. Before C_d determinations and after the cathodic pre-treatment, the TiO_2-NT samples were pre-cycled at 100 mV s^{-1} for 10 cycles to stabilize their response values.

$^{+}$/oxygen vacancies. The charge retention of all tested samples remained at 100% of faradaic efficiency (not shown) even after a long cycling process. Considering the morphology of TiO_2-NTs after the charge-discharge experiments, SEM images obtained after 5000 cycles showed that the nanotubular morphology was not altered for both thermal treatment methods, as showed in Fig. SC-9. The characteristic triangle shaped *E versus* time profiles, at varying current densities, of the TiO_2-NT electrodes thermally treated using a microwave oven and muffle furnace (see Fig. SC-10), confirmed that this material could be successfully used as supercapacitor.

3.3. Influence of the cathodic pre-treatment and thermally grown oxide over Ti

To analyze the near surface composition and bonding structure, *ex situ* XPS analysis was carried out for both types of samples, i.e. heat treated in microwave oven and muffle furnace. Fig. 6a shows that there is no significant difference between the Ti 2p spectra of both samples, showing the characteristic Ti $2p_{1/2}$ and Ti $2p_{3/2}$ spin orbit doublet centered at 458.7 and 464.5 eV, respectively, ascribed to the TiO_2 phase. No signal related to the Ti^{3+} oxidation state was observed for the analyzed samples, typically appearing as shoulder at 457.3 eV [41]. The O 1 s XPS spectra of Fig. 6b were fitted using three components related to Ti–O–Ti bonds, centered at 530.0 eV, surface Ti–OH hydroxide group at 531.3 eV and O–C bonds at 532.5 eV. The later component is related to oxidized surface contamination by adventitious carbon, frequently found also in *ex situ* measurements of reduced TiO_2-NT [19,20]. The principal difference in the O 1 s spectra observed for the two thermal treatments is the intensity increase (*ca.* 30%) of the Ti–OH

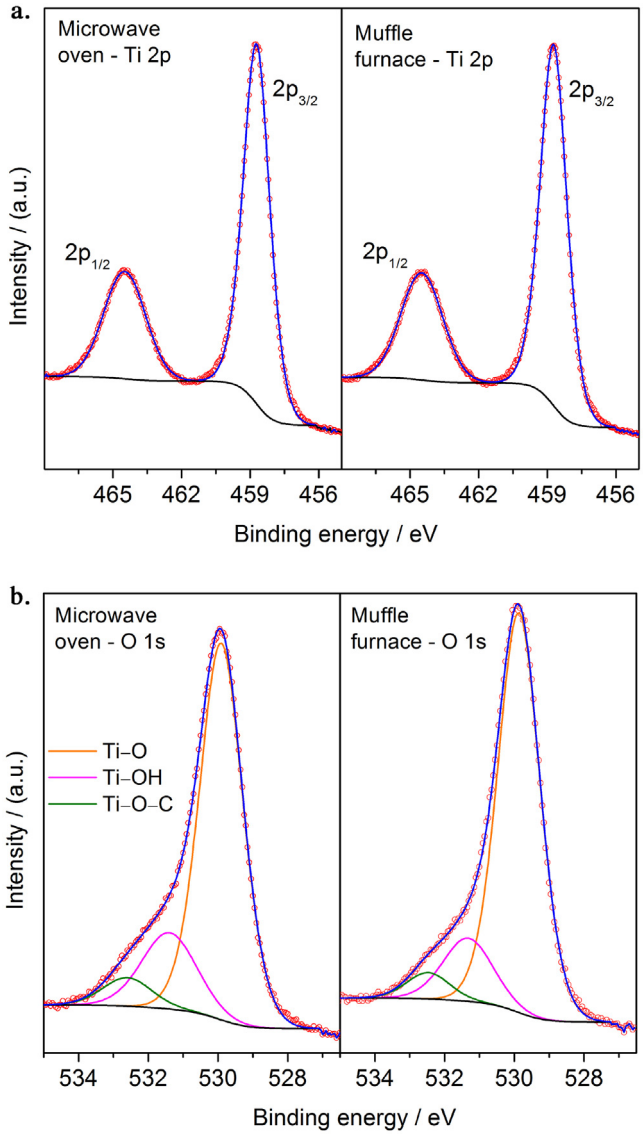

Fig. 6. XPS spectra of **a)** Ti 2p (○) and **b)** O 1 s orbitals (○) for TiO_2 samples heat treated in a microwave oven and muffle furnace after a cathodic pre-treatment (−1.4 V *vs.* NHE for 60 s). Colored lines refer to the fitting that was carried out (see text).

component for the microwave annealed sample. The higher amount of surface hydroxyl groups gives an indirect evidence for the increased amount of oxygen vacancies, and possibly also of Ti^{3+} species, on the surface of the TiO_2-NT film, which could originate from the rapid thermal cycle (only 3 min) of the microwave device. As discussed by Schaub et al. [27] and shown by Wendt et al. [28] through high-resolution scanning tunneling microscopy of reduced TiO_2 surfaces, oxygen vacancies dissociate adsorbed H_2O on the TiO_2 surface promoting a proton transfer to an adjacent oxygen atom. Thus, two hydroxyl groups for each oxygen vacancy are generated. Therefore, the higher amount of Ti–OH terminations on the surface of microwave annealed samples is an indirect proof of the superior generation of Ti^{3+}/oxygen vacancies in the near surface region after the cathodic pre-treatment. As reported by Zhang et al. [44], hydroxyls on the surface of TiO_2 can increase excess electrons on the Ti atoms and reduce their local valence, which may lead to shifts of the band edge of TiO_2 resulting in an increase of its reducing power for photocatalysis. Ganesh et al. [29] reported a diminishment of the oxidation barrier for the CO oxidation on hydroxylated surface of TiO_2. Clearly, surface hydroxylation of TiO_2 results in improved catalytic properties, such as the improved charge transfer found in this work (see below); however, the exact mechanism for this improvement needs to be further studied.

In order to investigate how the cathodic pre-treatment affects the electrical properties of the TiO_2-NT samples thermally treated using a microwave oven and muffle furnace, AC impedance measurements were carried out after the treatment and for distinct aging times (1 h to 156 h) in 0.5 mol L^{-1} Na_2SO_4 solution in the dark. Fig. 7 shows the charge transfer resistance (R_{ct}) and the areal capacitance of the constant phase element (*CPE*) evolution as a function of aging time in Na_2SO_4 solution after the cathodic pre-treatment, displayed as average value of three and four different TiO_2-NT samples for the microwave oven and muffle furnace, respectively, annealing methods. Electrochemical parameters, obtained by fitting the data using an equivalent circuit (inset of Fig. 7a) over the frequency spectrum are listed in Tables SC-3 to SC-7 of the supplementary content file. As can be inferred from Fig. 7a, the initial R_{ct} values (at 1 h after the cathodic pre-treatment) for the microwave annealed samples are slightly lower than that using a muffle furnace. That behavior might be due to the distinct amounts of reduced Ti^{3+}/oxygen vacancies in the crystalline structure of TiO_2, leading to a more conductive film for samples thermally treated using a microwave oven.

On the other hand, for longer aging times (>3 h; see Fig. 7a), the R_{ct} for the microwave oven annealed samples increased rapidly with a tendency for higher values than those of muffle furnace treated samples. Despite the higher amounts of Ti^{3+}/oxygen vacancies that might have been produced on the surface of microwave annealed samples, TiO_2-NT films that were heat treated in a muffle furnace seem to be capable to form a more conductive oxide film during water aging (see the distinct plateau of Fig. 7a). The R_{ct} increase during water aging is probably related to the scavenging effect of dissolved O_2 [45] in the electrolytic solution, towards the excess electrons on the TiO_2-NT surface. In addition, the areal capacitance of the CPE (with n values close to 1, see Table SC-5) for the microwave annealed TiO_2-NT is higher than that found for muffle furnace treated samples (Fig. 6b), which is in agreement with the results of galvanostatic charge-discharge experiments (Fig. 4). Another observation is that the capacitance values decreased slightly during water aging. That behavior might

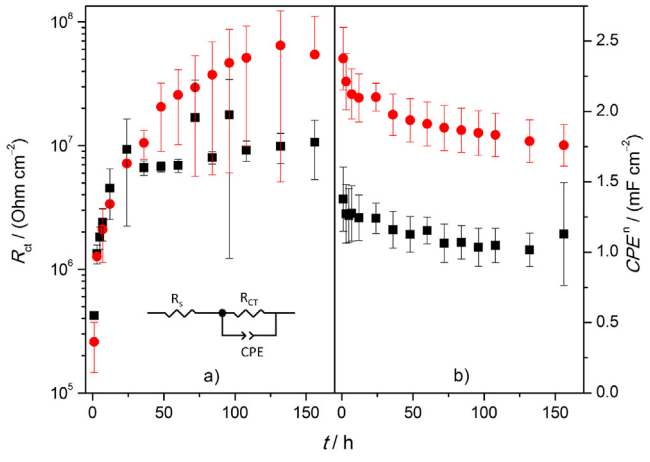

Fig. 7. a) Charge transfer resistance (R_{ct}) and b) areal capacitance of the constant phase element (CPE^n) evolution as a function of aging time (t) in 0.5 mol L^{-1} Na_2SO_4 solution after the cathodic pre-treatment (−1.4 V *vs.* NHE for 60 s) for TiO_2-NT samples heat treated using a (●) microwave oven (three repetitions) and (■) muffle furnace (four repetitions). The equivalent circuit used to fit data generated by electrochemical impedance spectroscopy is shown in the inset.

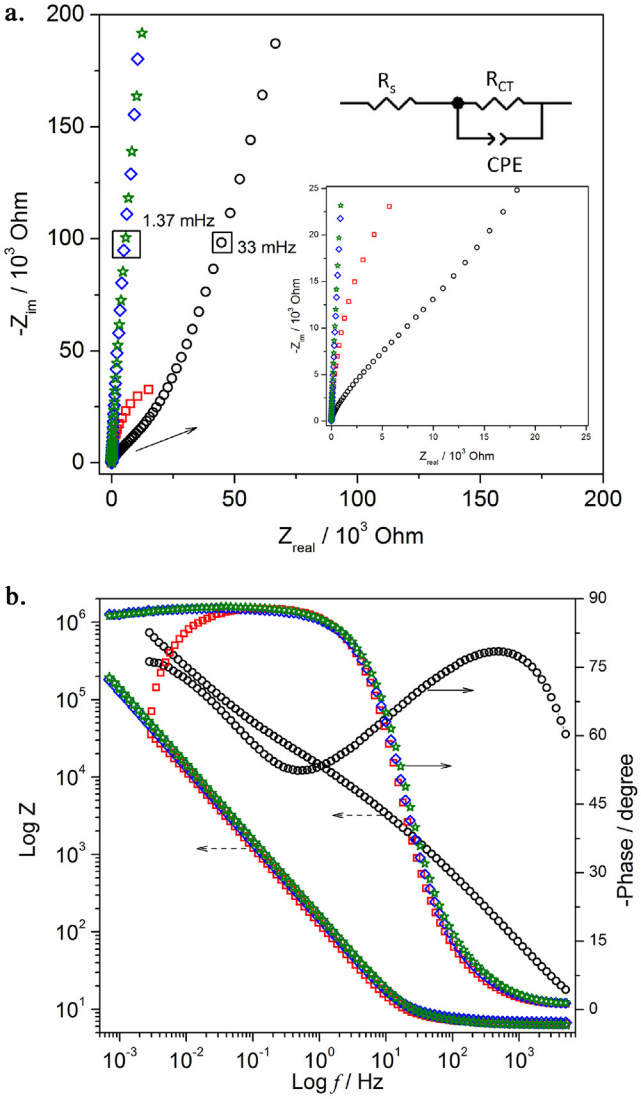

Fig. 8. a) Nyquist and **b)** Bode plots of TiO_2-NT samples heat treated in a microwave oven before (○) and after the cathodic electrochemical pre-treatment (−1.4 V *vs.* NHE for 60 s) for distinct aging times (□: 1 h; ◇: 72 h; ★: 156 h) in a 0.5 mol L^{-1} Na_2SO_4 solution. The equivalent circuit used to fit data generated by electrochemical impedance spectroscopy is shown in the inset of a).

be related to the increase of the charge transfer resistance of the TiO_2-NT.

Fig. 8 shows Nyquist and Bode plots for a microwave annealed TiO_2-NT sample at distinct aging times after the cathodic pre-treatment, as well as for the initial condition, i.e. before the electrochemical treatment. Clearly, the characteristic transmission line model of porous TiO_2-NT was changed to a simple electrochemical interface, as shown by the equivalent circuit in the inset of Fig. 8a and confirmed by the obtained profile of the phase angle of Fig. 8b, due to the conductivity increase of the TiO_2-NT film promoted by the electrochemical doping.

Finally, the influence of the thermally grown oxide (also called thermal barrier layer) at the interface between the TiO_2-NT and the Ti substrate was also investigated by AC impedance (from 10 kHz to 10 mHz) measurements. For such experiments, Ti plates (without previous anodization) were heat treated in the microwave oven and muffle furnace according to the time and temperature described in section 2. As already reported by Di Quarto and coworkers [46–48], depending on the temperature and time of the heat treatment, there is a variation of the thickness of the thermally grown oxide film, which can counteract to the good electric contact between the Ti and TiO_2-NT film, resulting in a high ohmic resistance that is deleterious for photocatalysis application. As can be seen in Fig. 9, the Nyquist and Bode plots were very similar for the thermally grown oxides using the microwave oven and muffle furnace. The equivalent circuit used to fit the experimental AC impedance data is shown in the inset of Fig. 9a. All fitting results obtained for the microwave oven and muffle furnace annealed samples are summarized in Tables SC-8 to SC-12, in the supplementary content file. The constant phase elements used in the equivalent circuit refer to the space charge capacitance of the thermally grown oxide (CPE_{SC}) semiconductor and to the double layer in solution (CPE_{DL}). The mean calculated charge transfer resistances (polarization resistance) of both thermally grown oxide were similar having values around 9 kΩ cm^{-2} (for six and five different samples of the microwave oven and muffle furnace annealing methods, respectively). Hence, as the electric parameters of the oxide barriers produced by both annealing methods are very close; they seem to have similar thickness and composition. This confirms that the distinct behavior of TiO_2-NT films observed for the areal capacitance and donor density by Mott-Schottky measurements, as well as the enhanced presence of hydroxyl groups found by XPS analyses, can be attributed to the rapid thermal cycle of microwave device and its effect on the TiO_2-NT film, i.e. the thermally grown oxide seem to not influence on those properties.

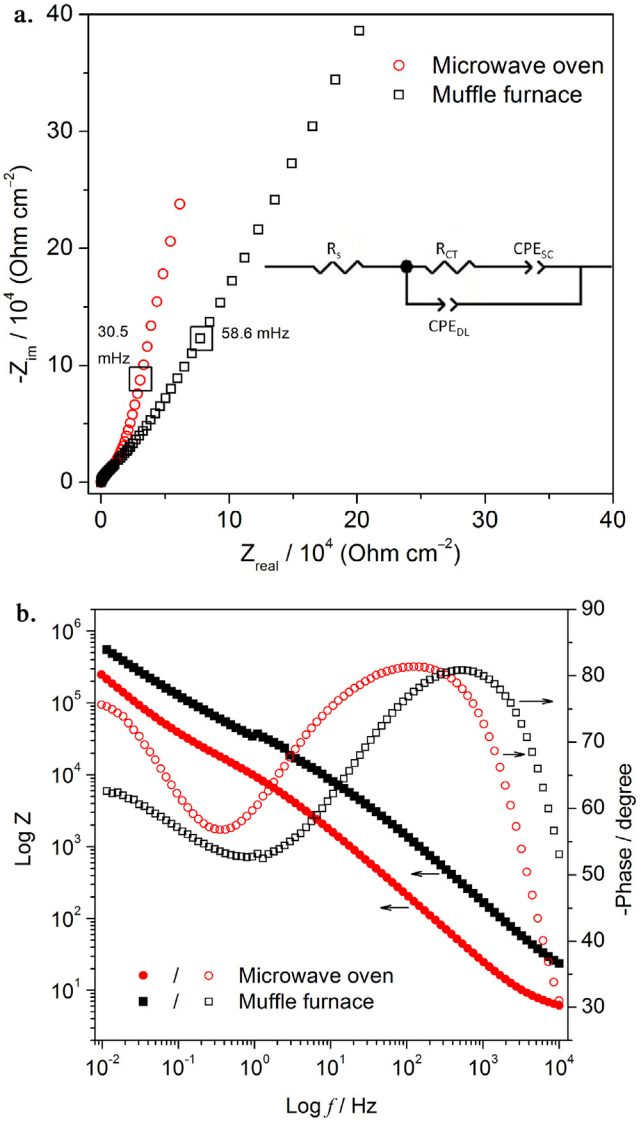

Fig. 9. a) Nyquist and **b)** Bode plots of Ti samples (without previous anodization) that were heat treated in a microwave oven and muffle furnace. The equivalent circuit used to fit data generated by electrochemical impedance spectroscopy is shown in the inset of a).

4. Conclusions

TiO_2 nanotube films annealed using a microwave oven exhibited similar morphological characteristics, mainly in the tube tops, than those annealed using a muffle furnace. No signal of the undesired rutile phase was observed and the characteristic values of band gap were found to be around 3 eV for both annealing methods. In addition, both annealed samples were successfully used as double layer supercapacitors (with high cycle stability), showing slightly higher values of areal capacitance for microwave annealed samples. This behavior is related with a more conductive nanotubular TiO_2 film after the cathodic electrochemical treatment, due to higher amounts of produced oxygen vacancies/Ti^{3+} in the anatase phase of the film, resulting in a higher hydroxylated surface for samples heat treated in microwave oven, as observed by X-ray photoelectron spectroscopy. In addition, no significant changes in the active surface area for samples heat treated by both methods were observed. On the other hand, stability tests carried out in the electrolytic solution (water aging) showed that the charge transfer resistance of the electrochemically reduced TiO_2 film annealed using a microwave oven increases more rapid than that using a muffle furnace, probably due to oxidation reaction with dissolved oxygen. The influence of the thermally grown oxide over Ti was not significant, as the electric parameters measured by AC impedance were very similar. All these findings show the importance and impact of different annealing techniques on the electrochemical properties of oxide materials.

Finally, the non-conventional thermal treatment method using a microwave is a rapid and easy procedure to convert amorphous TiO_2 nanotubes to the crystalline anatase phase, without any significant loss of morphological and electrical properties, which is important for the application of this material as supercapacitor.

Acknowledgements

Financial support and scholarships from the Brazilian funding agencies São Paulo Research Foundation –FAPESP (2012/13587-7), CAPES and CNPq are gratefully acknowledged. Prof. Ernesto C. Pereira (DQ-UFSCar) and Prof. Lucia Helena Mascaro Sales (DQ-

UFSCar) are also gratefully acknowledged for granting access to the UV-vis spectrometer.

Appendix A. Supplementary data

Supplementary data associated with this article can be found, in the online version, at http://dx.doi.org/10.1016/j.electacta.2017.05.112

References

[1] Q. Zhou, Z. Fang, J. Li, M. Wang, Applications of TiO_2 nanotube arrays in environmental and energy fields: A review, Microporous Mesoporous Mater. 202 (2015) 22–35.
[2] X. Wang, Z. Li, J. Shi, Y. Yu, One-dimensional titanium dioxide nanomaterials: Nanowires, nanorods, and nanobelts, Chem. Rev. 114 (2014) 9346–9384.
[3] K. Lee, A. Mazare, P. Schmuki, One-dimensional titanium dioxide nanomaterials: Nanotubes, Chem. Rev. 114 (2014) 9385–9454.
[4] D. Fattakhova-Rohlfing, A. Zaleska, T. Bein, Three-dimensional titanium dioxide nanomaterials, Chem. Rev. 114 (2014) 9487–9558.
[5] M. Nischk, P. Mazierski, Z. Wei, K. Siuzdak, N.A. Kouame, E. Kowalska, et al., Enhanced photocatalytic, electrochemical and photoelectrochemical properties of TiO_2 nanotubes arrays modified with Cu AgCu and Bi nanoparticles obtained via radiolytic reduction, Appl. Surf. Sci. 387 (2016) 89–102.
[6] S. Ananthakumar, J. Ramkumar, S.M. Babu, Semiconductor nanoparticles sensitized TiO_2 nanotubes for high efficiency solar cell devices, Renewable Sustainable Energy Rev. 57 (2016) 1307–1321.
[7] H. Zhou, X. Zou, Y. Zhang, Fabrication of TiO_2@MnO_2 nanotube arrays by pulsed electrodeposition and their application for high-performance supercapacitors, Electrochim. Acta 192 (2016) 259–267.
[8] A.E.R. Mohamed, S. Rohani, Modified TiO_2 nanotube arrays (TNTAs): Progressive strategies towards visible light responsive photoanode, a review, Energy Environ. Sci. 4 (2011) 1065.
[9] X. Zhou, N.T. Nguyen, S. Özkan, P. Schmuki, Anodic TiO_2 nanotube layers: Why does self-organized growth occur—A mini review, Electrochem. Commun. 46 (2014) 157–162.
[10] D. Yu, X. Zhu, Z. Xu, X. Zhong, Q. Gui, Y. Song, et al., Facile method to enhance the adhesion of TiO_2 nanotube arrays to Ti substrate, ACS Appl. Mater. Interfaces 6 (2014) 8001–8005.
[11] S. Rani, S.C. Roy, M. Paulose, O.K. Varghese, G.K. Mor, S. Kim, et al., Synthesis and applications of electrochemically self-assembled titania nanotube arrays, Phys. Chem. Chem. Phys. 12 (2010) 2780–2800.
[12] S. Das, R. Zazpe, J. Prikryl, P. Knotek, M. Krbal, H. Sopha, et al., Influence of annealing temperatures on the properties of low aspect-ratio TiO_2 nanotube layers, Electrochim. Acta 213 (2016) 452–459.
[13] A. Mazare, I. Paramasivam, F. Schmidt-Stein, K. Lee, I. Demetrescu, P. Schmuki, Flame annealing effects on self-organized TiO_2 nanotubes, Electrochim. Acta 66 (2012) 12–21.
[14] N. Liu, S.P. Albu, K. Lee, S. So, P. Schmuki, Water annealing and other low temperature treatments of anodic TiO_2 nanotubes: A comparison of properties and efficiencies in dye sensitized solar cells and for water splitting, Electrochim. Acta 82 (2012) 98–102.
[15] J.M. Aquino, R.C. Rocha-Filho, N. Bocchi, S.R. Biaggio, Microwave-assisted crystallization into anatase of amorphous TiO_2 nanotubes electrochemically grown on a Ti substrate, Mater. Lett. 126 (2014) 52–54.
[16] J.M. Aquino, J.P. Silva, R.C. Rocha-Filho, S.R. Biaggio, N. Bocchi, Comparison between microwave and muffle annealing of self-organized TiO_2 nanotubes into crystalline anatase, Mater. Lett. 167 (2016) 209–212.
[17] J.N. Hart, D. Menzies, Y.-B. Cheng, G.P. Simon, L. Spiccia, A comparison of microwave and conventional heat treatments of nanocrystalline TiO_2, Sol. Energy Mater. Sol. Cells 91 (2007) 6–16.
[18] S. Balaji, D. Mutharasu, N.S. Subramanian, K. Ramanathan, A review on microwave synthesis of electrode materials for lithium-ion batteries, Ionics 15 (2009) 765–777.
[19] H. Zhou, Y. Zhang, Electrochemically self-doped TiO_2 nanotube arrays for supercapacitors, J. Phys. Chem. C 118 (2014) 5626–5636.
[20] H. Zhou, Y. Zhang, Enhancing the capacitance of TiO_2 nanotube arrays by a facile cathodic reduction process, J. Power Sources 239 (2013) 128–131.
[21] K. Du, G. Liu, M. Li, C. Wu, X. Chen, K. Wang, Electrochemical reduction and capacitance of hybrid titanium dioxides—nanotube arrays and nanograss, Electrochim. Acta 210 (2016) 367–374.
[22] H. Zhang, Z. Chen, Y. Song, M. Yin, D. Li, X. Zhu, et al., Fabrication and supercapacitive performance of long anodic TiO_2 nanotube arrays using constant current anodization, Electrochem. Commun. 68 (2016) 23–27.
[23] X. Chen, L. Liu, F. Huang, Black titanium dioxide (TiO_2) nanomaterials, Chem. Soc. Rev. 44 (2015) 1861–1885.
[24] H.-S. Kim, J.B. Cook, H. Lin, J.S. Ko, S.H. Tolbert, V. Ozolins, et al., Oxygen vacancies enhance pseudocapacitive charge storage properties of MoO_{3-x}, Nat. Mater. 16 (2017) 454–460.
[25] Z. Li, Y. Ding, W. Kang, C. Li, D. Lin, X. Wang, et al., Reduction mechanism and capacitive properties of highly electrochemically reduced TiO_2 nanotube arrays, Electrochim. Acta 161 (2015) 40–47.
[26] J.M. Macak, B.G. Gong, M. Hueppe, P. Schmuki, Filling of TiO_2 nanotubes by self-doping and electrodeposition, Adv. Mater. 19 (2007) 3027–3031.
[27] R. Schaub, P. Thostrup, N. Lopez, E. Lægsgaard, I. Stensgaard, J.K. Nørskov, et al., Oxygen vacancies as active sites for water dissociation on rutile TiO_2(110), Phys. Rev. Lett. 87 (2001) 266104.
[28] S. Wendt, J. Matthiesen, R. Schaub, E.K. Vestergaard, E. Lægsgaard, F. Besenbacher, et al., Formation and splitting of paired hydroxyl groups on reduced TiO_2 (110), Phys. Rev. Lett. 96 (2006) 066107.
[29] P. Ganesh, P.R.C. Kent, G.M. Veith, Role of hydroxyl groups on the stability and catalytic activity of Au clusters on a rutile surface, J. Phys. Chem. Lett. 2 (2011) 2918–2924.
[30] L. Liu, P.Y. Yu, X. Chen, S.S. Mao, D.Z. Shen, Hydrogenation and disorder in engineered black TiO_2, Phys. Rev. Lett. 111 (2013) 065505.
[31] X. Chen, L. Liu, Z. Liu, M.A. Marcus, W.-C. Wang, N.A. Oyler, et al., Properties of disorder-engineered black titanium dioxide nanoparticles through hydrogenation, Sci. Rep. 3 (2013).
[32] G. Zhu, Y. Shan, T. Lin, W. Zhao, J. Xu, Z. Tian, et al., Hydrogenated blue titania with high solar absorption and greatly improved photocatalysis, Nanoscale 8 (2016) 4705–4712.
[33] J.P. Silva, S.R. Biaggio, N. Bocchi, R.C. Rocha-Filho, Practical microwave-assisted solid-state synthesis of the spinel $LiMn_2O_4$, Solid State Ionics 268 (2014) 42–47.
[34] D. Wang, L. Liu, F. Zhang, K. Tao, E. Pippel, K. Domen, Spontaneous phase and morphology transformations of anodized titania nanotubes induced by water at room temperature, Nano Lett. 11 (2011) 3649–3655.
[35] P. Acevedo-Peña, J.E. Carrera-Crespo, F. González, I. González, Effect of heat treatment on the crystal phase composition, semiconducting properties and photoelectrocatalytic color removal efficiency of TiO_2 nanotubes arrays, Electrochim. Acta 140 (2014) 564–571.
[36] S.P. Albu, H. Tsuchiya, S. Fujimoto, P. Schmuki, TiO_2 nanotubes –Annealing effects on detailed morphology and structure, Eur. J. Inorg. Chem. 2010 (2010) 4351–4356.
[37] R. López, R. Gómez, Band-gap energy estimation from diffuse reflectance measurements on sol–gel and commercial TiO_2: a comparative study, J. Sol-Gel Sci. Technol. 61 (2012) 1–7.
[38] C. Kim, S. Kim, J. Choi, J. Lee, J.S. Kang, Y.-E. Sung, et al., Blue TiO_2 nanotube array as an oxidant generating novel anode material fabricated by simple cathodic polarization, Electrochim. Acta 141 (2014) 113–119.
[39] M. Nowak, B. Kauch, P. Szperlich, Determination of energy band gap of nanocrystalline SbSI using diffuse reflectance spectroscopy, Rev. Sci. Instrum. 80 (2009) 0461071–0461072.
[40] D.L. Wood, J. Tauc, Weak absorption tails in amorphous semiconductors, Phys. Rev. B 5 (1972) 3144–3151.
[41] U. Diebold, The surface science of titanium dioxide, Surf. Sci. Rep. 48 (2003) 53–229.
[42] A. Ghicov, H. Tsuchiya, R. Hahn, J.M. Macak, A.G. Muñoz, P. Schmuki, TiO_2 nanotubes: H^+ insertion and strong electrochromic effects, Electrochem. Commun. 8 (2006) 528–532.
[43] A. Naldoni, M. Allieta, S. Santangelo, M. Marelli, F. Fabbri, S. Cappelli, et al., Effect of nature and location of defects on bandgap narrowing in black TiO_2 nanoparticles, J. Am. Chem. Soc. 134 (2012) 7600–7603.
[44] D. Zhang, M. Yang, S. Dong, Hydroxylation of the rutile TiO_2(110) surface enhancing its reducing power for photocatalysis, J. Phys. Chem. C 119 (2015) 1451–1456.
[45] S.H. Szczepankiewicz, A.J. Colussi, M.R. Hoffmann, Infrared spectra of photoinduced species on hydroxylated titania surfaces, J. Phys. Chem. B 104 (2000) 9842–9850.
[46] S. Miraghaei, F. Ashrafizadeh, K. Raeissi, M. Santamaria, F. Di Quarto, An electrochemical investigation on the adhesion of as-formed anodic TiO_2 nanotubes grown in organic solvents, Electrochem. Solid-State Lett. 14 (2011) K8–K11.
[47] S. Miraghaei, F. Ashrafizadeh, M. Santamaria, F. Di Quarto, K. Shimizu, Influence of anodic and thermal barrier layers on physicochemical behavior of anodic TiO_2 nanotubes, J. Electrochem. Soc. 158 (2011) K197–K204.
[48] M. Santamaria, G. Conigliaro, F. Di Franco, B. Megna, F. Di Quarto, Electronic properties of thermal oxides on Ti and their influence on impedance and photoelectrochemical behavior of TiO_2 nanotubes, J. Electrochem. Soc. 164 (2017) C113–C120.